

# Remanence deviations in permanent magnet synchronous machines evaluated using a model order reduction approach

Johann Kolb  | Fabian Müller | Kay Hameyer

Institute of Electrical Machines (IEM),  
RWTH Aachen University, Aachen,  
Germany

## Correspondence

Johann Kolb, Institute of Electrical  
Machines (IEM), RWTH Aachen  
University, Schinkelstr. 4, Aachen 52062,  
Germany.  
Email: [johann.kolb@iem.rwth-aachen.de](mailto:johann.kolb@iem.rwth-aachen.de)

## Funding information

German Research Foundation,  
Grant/Award Numbers: 347941356,  
323896285

## Abstract

In this article remanence deviations of a permanent magnet synchronous machine are studied with the proper orthogonal decomposition (POD). The design of experiments enables to create designs with a reduced sample size compared to full factorial designs without decreasing the stochastic significance of the remanence distributions. Next, a POD basis is created with the belonging design, that is distinctly smaller than the reference. From the POD basis the projection matrix is built to compute the flux density solutions. The machine's output is then analyzed regarding accuracy originating from numerical errors. Different parameters are evaluated and compared to the reference to appraise the accuracy of the flux density solutions, which includes the POD basis size, rotor angle step size and dimension of the reduced system. Results show, that the most influence has the dimension of the reduced system. Depending on the dimension and other parameters about one quarter of computational effort can be conserved without a significant loss in accuracy.

## KEYWORDS

design of experiments, model order reduction, permanent magnet synchronous machine, proper orthogonal decomposition, remanence deviations

## 1 | INTRODUCTION

In electrical machines, large numbers of manufacturing tolerances could influence the output behavior of the machine. One approach to study an effect in detail is the one-factor-at-a-time (OAT) analysis, another approach is design of experiments (DOE), where combined effects of manufacturing tolerances are analyzed.<sup>1</sup>

With DOE the sample size, which determines the simulation effort, is reduced to a minimum without decreasing the result's significance.<sup>1</sup> But even with a reduced sample size, a lot of finite element (FE) simulations are required by the analysis. In addition, for the investigation of manufacturing tolerances a full-size FE-model has to be simulated to vary all individual tolerances independently. In a previous sensitivity analysis different reduction strategies on the model and the analysis were applied to cope the simulation effort.<sup>2</sup>

While the sample size is minimized with DOE, the only further way to reduce the simulation effort is to employ a model order reduction (MOR) within the FE simulation. In different studies MOR methods have been applied to

This is an open access article under the terms of the [Creative Commons Attribution-NonCommercial](https://creativecommons.org/licenses/by-nc/4.0/) License, which permits use, distribution and reproduction in any medium, provided the original work is properly cited and is not used for commercial purposes.

© 2022 The Authors. *International Journal of Numerical Modelling: Electronic Networks, Devices and Fields* published by John Wiley & Sons Ltd.

electrical machines to reduce the DOF and as a consequence the simulation effort.<sup>3,4</sup> Furthermore, DOE and MOR has been combined for optimization, but not for analyzing manufacturing tolerances.<sup>5</sup> Therefore, this study analyzes the accuracy of the combination of DOE and MOR for manufacturing tolerances in electrical machines.

For a permanent magnet synchronous machine, the sensitivity analysis is conducted exemplarily as manufacturing tolerance analysis of the permanent magnets, where the distribution of the remanent magnetic flux density is known. Hereby, a DOE parameter space is created, that includes all magnets with its representative distributions. Subsequently, the simulations are performed with the indicated technique and compared to conventional simulations as reference while utilizing the same DOE samples. In contrast, the POD basis is created with a distinct smaller sample size.

As comparison criteria the mean torque, torque ripple and the radial force excitation are calculated for POD and reference. The differences of the accuracy are outlined with the distributions of the comparisons criteria, as well as the successive characterizing factors including mean value and standard deviation. Moreover, the computational effort is evaluated to show the advantages of combining POD and DOE.

## 2 | FUNDAMENTALS

The simulation of electrical machine is commonly conducted by finite element analysis (FEA). Particularly, for the computation of synchronous machines, which do not utilize transient effects as fundamental working principle, it is possible to use magnetostatic formulations. In this research the magnetostatic vector potential formulation is employed, which origins from Ampères law in combination with a vectorial magnetic potential  $\mathbf{A}$  and reasonable material model with reluctivity  $\nu$ . It is assumed, that the eddy currents in the permanent magnets can be neglected as well as in the flux guiding material, which is usually made of thin electrical steel sheets. As excitation the current density  $\mathbf{J}$  and magnetic flux density of the magnets  $\mathbf{B}_R$  are considered.

$$\nabla \times \nu \nabla \times \mathbf{A} = \mathbf{J} + \nabla \times \nu \mathbf{B}_R. \quad (1)$$

From the magnetic vector potential the flux density is derived

$$\mathbf{B} = \nabla \times \mathbf{A}. \quad (2)$$

Finally, to be able to simulate arbitrary rotor positions a sliding interface technique is applied.<sup>6</sup> The discretization of the problem geometry is directly related to the degrees of freedom.

In this study, three different quality objectives are defined to compare the accuracy of the solutions which are based on the force density at rotor and stator. From the magnetic flux density solution the force density  $\sigma_F(\alpha, t)$  is derived at spatial angle  $\alpha$  and time  $t$ . Subsequently, the force density is split into the tangential  $\sigma_{Ftan}(\alpha, t)$  and radial force density  $\sigma_{Frad}(\alpha, t)$ . Thus, the torque of the machine at time  $t$  is given by

$$T(t) = r_R^2 l \int_0^{2\pi} \sigma_{Ftan}(\alpha, t) d\alpha \quad (3)$$

with rotor radius  $r_R$  and machine length  $l$ . The mean torque is calculated over the time period  $\tau$  for one mechanical revolution of the rotor.

$$\bar{T} = \frac{1}{\tau} \int_0^\tau T(t) dt. \quad (4)$$

The torque ripple is defined as the average distance from maximum and minimum peak to mean torque for a revolution.

$$T_R = \frac{\max(T(t)) - \min(T(t))}{2\bar{T}}. \quad (5)$$

The excitation of the stator that induce vibrations in the machine housing is mainly influenced by the air gap radial forces. To estimate the manufacturing deviations, the variance of the radial forces  $\sigma_{\text{rad}}^2$  is calculated over all spatial  $s$  and temporal  $r$  modes except the constant component

$$\sigma_{\text{rad}}^2 = \frac{1}{2} \sum_{s=1}^{\infty} \sum_{r=1}^{\infty} (A_{\text{sr}}^2 + B_{\text{sr}}^2), \quad (6)$$

where  $A_{\text{sr}}$  and  $B_{\text{sr}}$  represent the two-dimensional complex Fourier coefficients of the force density  $\sigma_{\text{Frad}}$ .<sup>2</sup>

## 2.1 | Proper orthogonal decomposition

The consistent strive for reducing the computational time of numerical simulations can be addressed by model order reduction techniques. In recent times methods such as the proper orthogonal decomposition (POD) gained particular popularity in the simulation of electromagnetic fields. In general, the POD is based on exploiting the solution subspace. The projection operator used in the POD is then utilized to achieve a reduced system, holding much fewer DOF, in which the solution is approximated.<sup>7</sup> The reduced form is achieved by extracting information of the subspace from already computed solutions.

$$\mathbf{M}_S = \mathbf{V}\Sigma\mathbf{W}. \quad (7)$$

For this purpose the solutions are assembled in a matrix and separated into singular vectors by a singular value decomposition (SVD) (7). The left singular vectors given in  $\mathbf{V}$  are then used to span an orthogonal base in the solution subspace. Furthermore, the basis is truncated by assessing the information content of each singular vector given by the singular values, contained in  $\Sigma$ . Finally, this base is used to map the reference system of dimension DOF into a system of reduced order  $m$  and is also referred to as projection matrix  $\Psi$ .<sup>3,8</sup>

$$\Psi^T \mathbf{M} \Psi \Psi^T \mathbf{X} = \Psi^T \mathbf{B}. \quad (8)$$

$X$  is here the solution vector of the magnetic vector potential, which depends on all excitation parameters as well as the rotor position. As a direct consequence of the fundamental principle of POD, the solutions, also referred to as snapshots and used to create the projection matrix, have a large influence on the accuracy of the reduced model. In recent research, different approaches for the snapshot selection are studied and a distinct influence of the snapshot selection on the accuracy of the solution is found.<sup>9</sup> With focus on the simulation of electrical machines involving motion, it is reasonable to spread the snapshots in evenly distributed rotor positions in the interval of interest, for example, a mechanical revolution.<sup>10</sup> The POD, as a model order reduction technique, can be used to cope with the computational burden of repetitive solving of large systems of equations with many degrees of freedom. The technique reduces the system of size (DOF  $\times$  DOF) into a small system with a size equal or less than the number of snapshots.<sup>7</sup>

In Figure 1 are the first three singular vectors  $\Psi_i$  given for an exemplary synchronous machine. The snapshots in this example are taken from a locked rotor simulation and the sum of weighted singular vectors approximates the solutions in the reference system (9). The weighting factors are the entries of the reduced solution vector  $\mathbf{X}_r$

$$\mathbf{X} = \Psi \mathbf{X}_r. \quad (9)$$

## 2.2 | Design of experiments

To evaluate the distribution of the quality objectives, a uniformly distributed parameter space is necessary, where subsequently the parameter distributions are comprised into for an accurate evaluation of the machine's output. With DOE, it is possible to create designs with a minimized sample size without forfeit accuracy compared to a full factorial design.

Recent research has studied the probability errors for large quasi-Monte Carlo (QMC) methods and obtained as a result, that Sobol sequences yield to smaller errors than other methods, for example, Latin hypercube sampling or Halton sequences.<sup>11,12</sup> Therefore, for the creation of the uniformly distributed parameter space Sobol sequences are

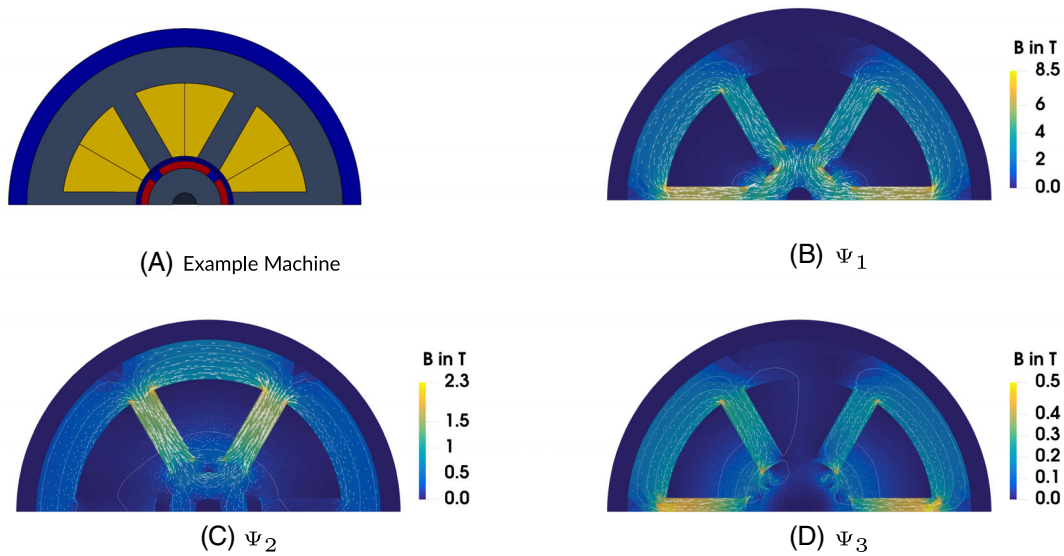


FIGURE 1 Example machine and associated singular vectors contained in  $\Psi$  (9)

used. The Sobol sequences are based on a bit-wise calculation, starting with a polynomial and recombination of a bit-wise exclusive or operations on the polynomial coefficients, so that the discrepancy between each sample  $x$  in the sequence  $S$  is minimized.<sup>13</sup>

To consider the distribution of the input parameters different distribution types can be utilized. This study entails only normal distributions, thus the probability density is described as

$$p(x) = \frac{1}{\sqrt{2\pi\sigma^2}} \exp\left(-\frac{(x-\mu)^2}{2\sigma^2}\right) \quad (10)$$

with the mean  $\mu$  and the standard deviation  $\sigma$ . The cumulative distribution function of the probability density is derived with

$$P(x) = \int_{-\infty}^x p(\tau) d\tau. \quad (11)$$

To comprise the probability distribution into the DOE, the resulting Sobol sequences are modified by scaling the sequences with the inverse cumulative distribution function.<sup>14</sup>

$$x_p = P(x)^{-1}. \quad (12)$$

The resulting sequence  $S_p$  with the samples  $x_p$  builds the parameter space for the reference as well as the POD simulations.

### 3 | SIMULATION

For this study a permanent magnet synchronous machine is utilized, which was previously analyzed concerning drive simulation and manufacturing tolerances.<sup>2,15</sup> The rated power of the machine is 4.5 kW with a rated speed of 4450 rpm and a torque of 9.6 Nm. The simulations are performed at the rated operating current of  $I = 10$  A. Moreover it has fractional slot windings ( $q = 0.5$ ) and 12 buried magnets. Figure 2 outlines the cross section of the machine as well as the

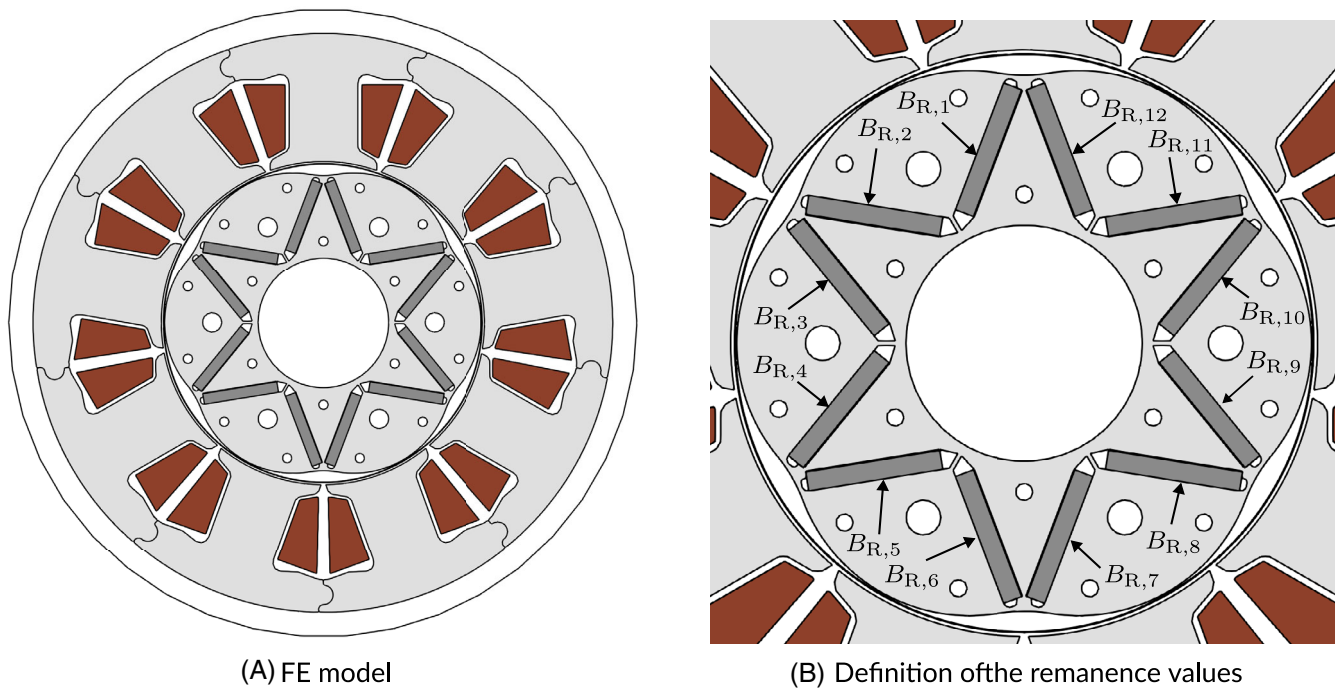


FIGURE 2 Cross section of the machine

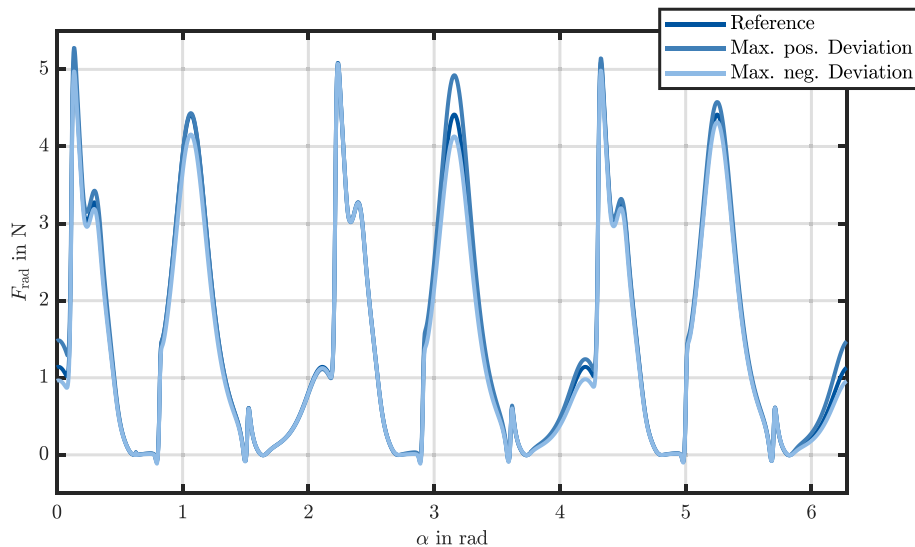


FIGURE 3 Radial airgap forces at its reference state and with the overall maximum remanence deviation in positive and negative direction from design of experiments

definition of the remanent magnetic flux density values  $B_R$  of each magnet, which are assumed to be homogeneous in each magnet.

As this study focuses on the magnets, the individual tolerance distributions of all magnets are considered. The mean of the remanence is  $B_R = 1.25$  T and the tolerance limits are defined as 1.1 and 1.4 T. The tolerance limit is set here as the  $3\sigma$  border of a normal distribution. Therefore the standard deviation is given by  $\sigma = 0.05$  T.

A DOE with 200 samples is built, which consists of a parameter space with the 12 remanences mentioned. The Chi-squared test, which calculates the goodness of fit for a distribution, reveals a significance level of greater than 99.99% for the parameter space, so that the discretization of the distribution does not affect the distribution of the quality objectives.<sup>16</sup> An individual dimension  $i$  of the DOE parameter space is assigned to a remanence value  $B_{R,i}$  of the machine.

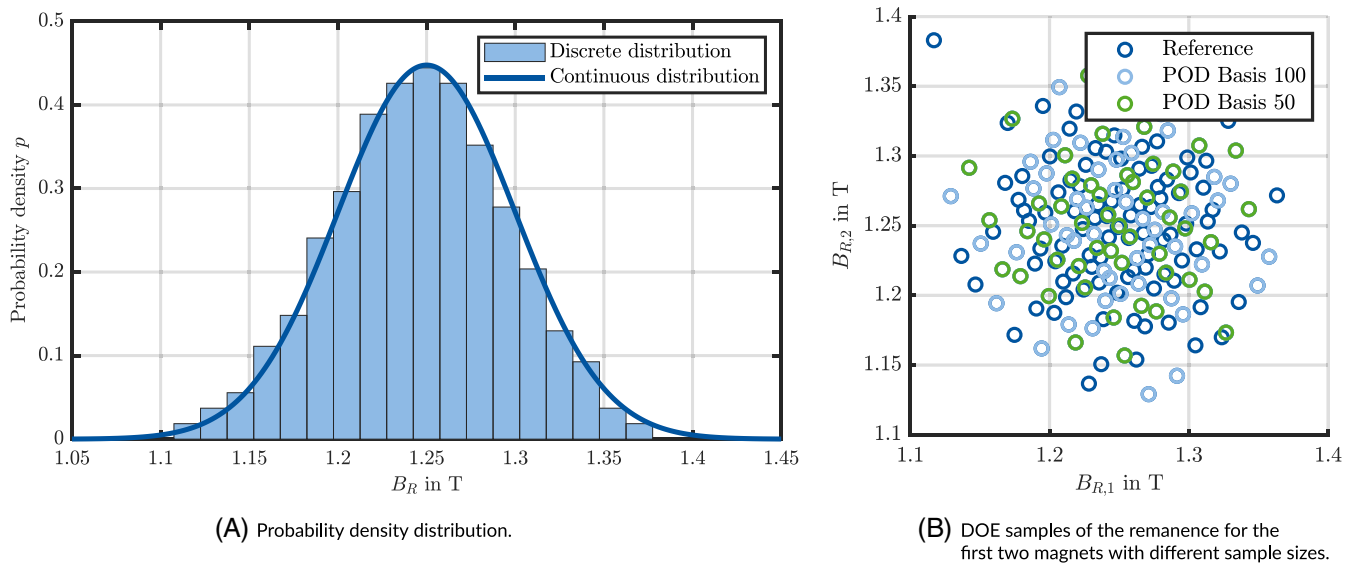


FIGURE 4 Distribution of the magnet's remanence

Figure 4A shows the predefined continuous probability density (10) and the discrete distribution as output of the DOE sequence. Figure 3 indicates the radial airgap forces over the spatial angle  $\alpha$  at its reference state and the simulated samples with the maximum positive and negative remanence deviation. Because the magnets have individual remanence values, the difference in radial and tangential forces compared to the reference can vary from one pole to another, which is visible in the figure at the peak values at  $\alpha = 1.1$ ,  $\alpha = 3.2$ , and  $\alpha = 5.2$  rad.

Thus, the simulation cannot be performed as a partial model and a full model has to be applied. First, reference simulations are conducted to compare and evaluate the accuracy of the POD solutions. For comparison, the three quality objectives, mentioned in Section 2, are determined for a mechanical revolution of the rotor.

For the POD basis, from which the projection matrix is calculated, two different designs are built with DOE, that cover the same parameter space while keeping the distribution. The first POD basis has 50 and the second one 100 samples, which are 25% and 50% of the reference design size, respectively. Figure 4B outlines the correlation of the DOE samples between the first two magnets for the reference, POD basis 50 and POD basis 100 design.

A significant factor for the accuracy of the POD simulations could be the resolution between each flux density solution from which the projection matrix is calculated. Therefore also the step size for one mechanical revolution is varied, which are 120, 180 and 360, so that the angle difference is  $\Delta\gamma = 3.0^\circ$ ,  $\Delta\gamma = 2.0^\circ$ , and  $\Delta\gamma = 1.0^\circ$ .

Also the dimension of the reduced system is analyzed. As first option, the projection matrices are set to a size that is equal to the step size. As second option, a truncation threshold of 0.02 is set, so that for the POD basis 50 the results of 50 sample simulations for one revolution with the according number of angular steps are utilized to create the projection operator. For example, the POD basis 50 and an angular step size of  $\Delta\gamma = 3.0^\circ$  result in a total number of snapshots of  $50 \times 120 = 6000$  and with the truncation threshold the dimension of the truncated projection operator is reduced to 22. As a result, with the truncation threshold the number of singular vectors contained in the projection matrix is reduced to 22 instead of 120 in the first option.

To evaluate the accuracy of the different options, at first the POD bases for both sample sizes are computed with the FE-solver. Second, the projection matrices are created for the specific sample sizes, angular step size and the dimension of the reduced system. At last, the flux density solutions are computed with the belonging projection matrices with the same DOE samples, that were provided for the reference solutions, so that with the 200 samples the DOE resolution remains equal and is comparable.

## 4 | EVALUATION

The evaluation relies on the quality objectives mean torque, torque ripple and the variance of the radial forces. The reference mean output for all three quality objectives is hereby outlined as 100% to give a better understanding of the

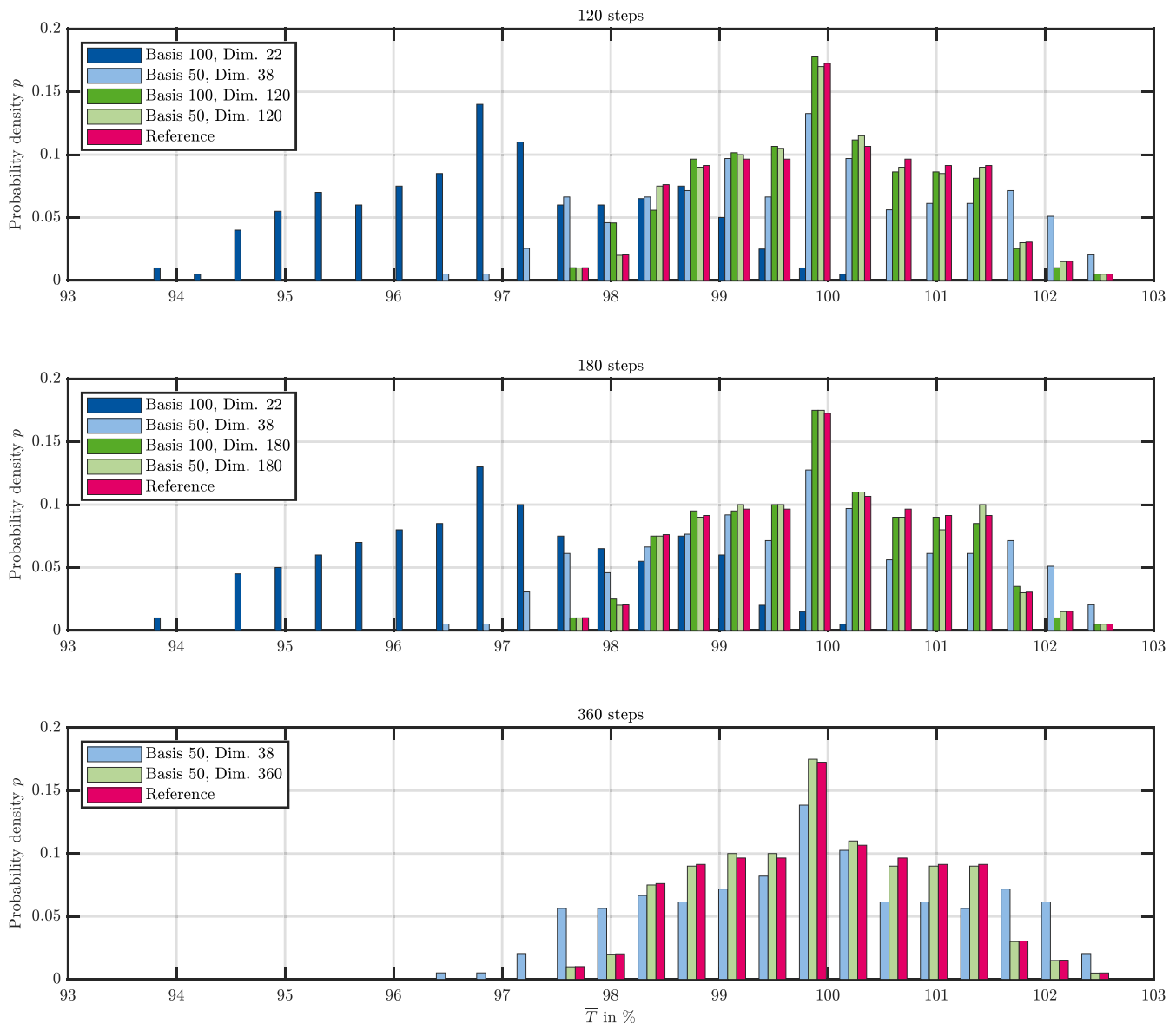


FIGURE 5 Distribution of the mean torque

deviation. All figures show the probability density distributions dependent on the POD basis sizes, dimension of the reduced system and the step sizes. Due to hardware limits it is not possible to compute the projection matrices for an angular step size of 360 with a POD basis of 100.

Figure 5 denotes the results for the calculated mean torque. The output of the reference design varies between 97.5% and 102.5%. For a POD basis size of 50 and 100 with a dimension equal to the step size, the distribution is close to the reference with small deviations in the probability density. The results with a POD basis 50 with a dimension of 38 have a slightly higher deviation of about 1%. The distribution of POD basis 100 with a dimension of 22 by contrast has its mean at 96.8% and an even higher deviation. A significant difference between the step sizes is not visible.

The evaluation of the torque ripple in Figure 6 reveals further deviations and differences for the different DOE simulations. The reference deviates between 98% and 103.5%. The POD bases equal to the step sizes closely correlates with the reference, however the results for the POD basis 50 at 120 steps possesses a higher mean than the reference and POD basis 100. While the POD basis 50 with a dimension of 38 shows a distinct higher mean between 107% and 113%, the POD basis 100 with 22 singular vectors has a mean between 88% and 89% with an even higher deviation.

The variance of the radial forces in Figure 7 indicates a similar behavior as the torque ripple. The results for POD basis 50 and 100 with a dimension size equal to the step size coincide with the reference, only the mean of POD basis

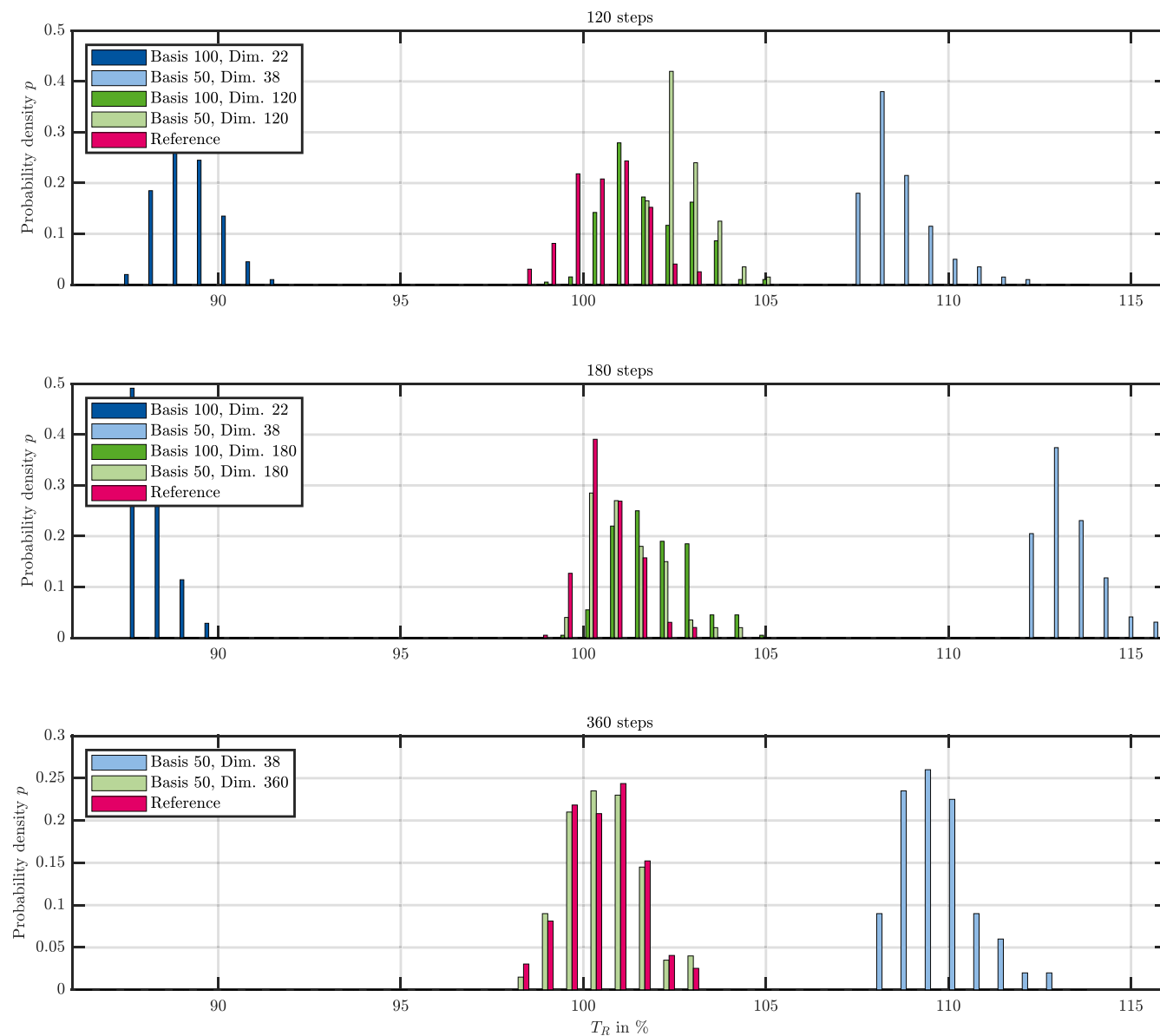


FIGURE 6 Distribution of the torque ripple

50 at 120 steps is 2% higher. The result of POD basis 50 with 38 singular vectors has a significant higher deviation, a distinct mean is not clearly visible. The result of POD basis 100 with a dimension of 22 snapshots expose the mean between 88% and 89% with an even more distinct deviation.

As a result from the different simulations deduced with the evaluation, the influence of the number of the singular vector is significantly more important than the POD basis size or the angular step size. The discretization of the steps and distributions with DOE can be a factor, if the angular step difference is further increased than in this study.

Another important factor addresses the computational effort as an additional measure for the efficiency of the POD technique. In Figure 8 the computational time of the reference simulations is set to 100%, so that the savings potential with the POD technique for the different evaluations becomes visible. The computational effort includes the computational time for the POD basis simulations, the projection matrices calculation as well as the flux density computation with the reduced system. All simulations were performed on the same hardware, so that the computational effort is adequately comparable.

The computational effort for the step size of 120 and 180 is nearly similar with a saving between 22% and 46% at maximum. For 360 steps the computational effort increases for POD basis 50 and an equal step size up to the computational time of the reference. Overall, the computational effort for the POD basis 50 is significantly higher when



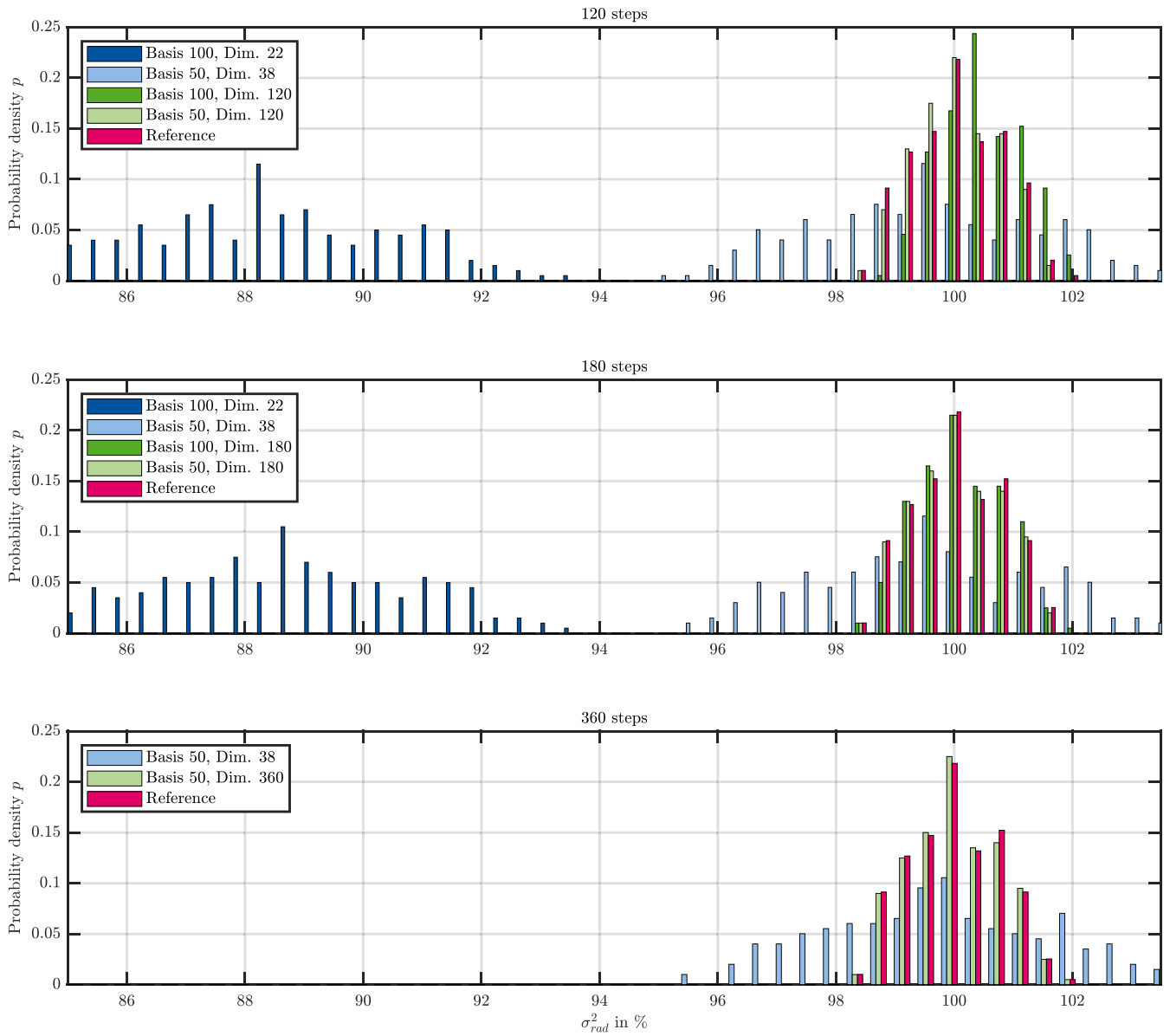


FIGURE 7 Distribution of the radial force variance

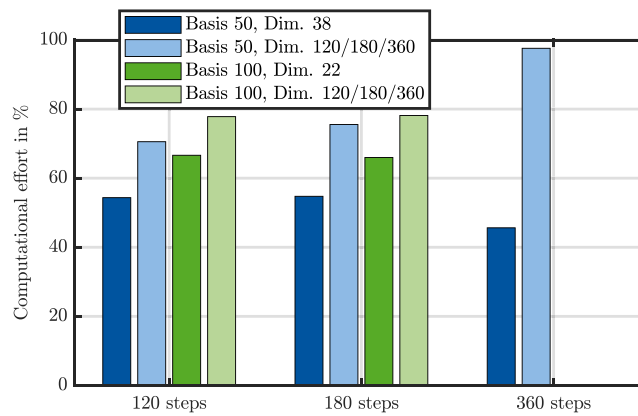


FIGURE 8 Computational effort relative to reference simulations

increasing the size of the projection matrix (up to 22% higher) while the difference for the POD basis 100 calculations remains smaller with a difference of about 10%. Regarding the overall efficiency without a significant accuracy loss and a valuable saving of the computational effort, the POD basis size of 50 with a step size of 180 is the best choice here.

But even the computational savings are high, there are various improvements to speed up the implementation, for example, reducing the copy procedures of the system matrices in the memory. Another numerical approach to further minimize the computational effort is the reduction via POD and discrete empirical interpolation method (DEIM).<sup>17</sup>

## 5 | CONCLUSIONS

In this study, the POD is employed as a reduction technique to evaluate the accuracy of remanence deviations in a permanent magnet synchronous machine relative to a reference for manufacturing tolerance analysis. With DOE in the first part designs with minimized sample sizes are created that contain the remanent magnet flux density deviations for all 12 magnets. In the second part, POD bases are generated with the belonging design, that are a part of the reference size. From the POD bases the projection matrices are built to compute the flux density solutions. At last from the force density the mean torque, torque ripple, and variance of the radial forces as quality objectives are calculated.

To appraise the accuracy of the POD technique, the dimension of the reduced system, POD basis and angular step size of one mechanical revolution is varied. As a result, the most influence of the remanence deviation on the quality objective distributions has the dimension of the singular vectors and therefore the size of the projection operator. Increasing the dimension reduces the displacement of the quality objectives between reference and POD as well as the deviation of the distribution while saving 22% computational effort at minimum. The POD basis and the angular step size have minor influences on the accuracy, but can further reduce the computational effort. In contrast, an angular step distance chosen too small combined with a high-dimensional projection matrix does not increase furthermore the accuracy, but can give away the advantage of a computational effort saving.

This study reveals, that even a small POD dimension is able to capture the most dominant information of the parameter variation on the machine's output behavior. With DOE and POD applied in the design or analyzing process of electrical machines, manufacturing tolerances can be considered with less computational effort than conventional FE-simulations.

## ACKNOWLEDGEMENTS

This work was supported by the German Research Foundation (DFG) within the research project number 323896285 "Propagation of uncertainties across electromagnetic models" and within the research project number 347941356 "Numerical Analysis of Electromagnetic Fields by Proper Generalized Decomposition in Electrical Machines". Open Access funding enabled and organized by Projekt DEAL.

## DATA AVAILABILITY STATEMENT

Research data are not shared.

## ORCID

Johann Kolb  <https://orcid.org/0000-0003-3442-7830>

## REFERENCES

1. Saltelli A, Ratto M, Andres T, et al. *Global Sensitivity Analysis: the Primer*. Wiley; 2008.
2. Kolb J, Hameyer K. Sensitivity analysis of manufacturing tolerances in permanent magnet synchronous machines with stator segmentation. *IEEE Trans Energy Convers*. 2020;35(4):2210-2221.
3. Hasan MR, Montier L, Henneron T, Sabariego RV. Stabilized reduced-order model of a non-linear Eddy current problem by a Gappy-POD approach. *IEEE Trans Magn*. 2018;54(12):1-8.
4. Farzamfar M, Rasilo P, Martin F, Belahcen A. Proper orthogonal decomposition for order reduction of permanent magnet machine model. Proceedings of the 18th International Conference on Electrical Machines and Systems (ICEMS); 2015; IEEE.
5. Renganathan SA, Maulik R, Rao V. Machine learning for nonintrusive model order reduction of the parametric inviscid transonic flow past an airfoil. *Phys Fluids*. 2020;32(4):047110.
6. Lange E, Henrotte F, Hameyer K. A Variational formulation for nonconforming sliding interfaces in finite element analysis of electric machines. *IEEE Trans Magn*. 2010;46(8):2755-2758.

7. Henneron T, Clénet S. Model order reduction of non-linear Magnetostatic problems based on POD and DEI methods. *IEEE Trans Mag*. 2014;50:33-36.
8. Montier L, Henneron T, Clénet S, Goursaud B. Transient simulation of an electrical rotating machine achieved through model order reduction. *Adv Model Simul Eng Sci*. 2016;46:10.
9. Müller F, Crampen L, Henneron T, Clénet S, Hameyer K. Model order reduction techniques applied to magnetodynamic scalar potential formulation. Proceedings of the 2019 19th International Symposium on Electromagnetic Fields in Mechatronics, Electrical and Electronic Engineering (ISEF); 2019; IEEE.
10. Müller F, Siokos A, Kolb J, Nell M, Hameyer K. Efficient estimation of electrical machine behavior by model order reduction. *IEEE Trans Magn*. 2021;57(6):1-4.
11. Wang X, Sloan IH. Low discrepancy sequences in high dimensions: how well are their projections distributed? *J Comput Appl Math*. 2008;213(2):366-386.
12. Niederreiter H. *Random Number Generation and Quasi-Monte Carlo Methods*. Society for Industrial and Applied Mathematics; 1992.
13. Bratley P, Fox BL. Algorithm 659: implementing Sobol's Quasirandom sequence generator. *ACM Trans Math Softw*. 1988;14(1):88-100.
14. Royston JP, Algorithm AS. 177: expected Normal order statistics (exact and approximate). *J R Stat Soc Ser C Appl Stat*. 1982;31(2): 161-165.
15. Schmuelling S, Drubel O, Ummelmann R, de Zeeuw M. Combined method for simulation of high efficient circulating pumps. Proceedings of the 2016 XXII International Conference on Electrical Machines (ICEM); 2016:212-217; IEEE.
16. Cochran WG. The  $\chi^2$  test of goodness of fit. *Ann Math Stat*. 1952;23(3):315-345.
17. Ghavamian F, Tiso P, Simone A. POD-DEIM model order reduction for strain-softening viscoplasticity. *Comput Methods Appl Mech Eng*. 2017;317:458-479.

**How to cite this article:** Kolb J, Müller F, Hameyer K. Remanence deviations in permanent magnet synchronous machines evaluated using a model order reduction approach. *Int J Numer Model*. 2022;e3062. doi:[10.1002/jnm.3062](https://doi.org/10.1002/jnm.3062)